⌘ *Author's Choice*
THE JOURNAL OF BIOLOGICAL CHEMISTRY VOL. 290, NO. 13, pp. 8039–8047, March 27, 2015

HCO_3^--independent pH Regulation in Astrocytes *in Situ* Is Dominated by V-ATPase*◆

Received for publication, January 6, 2015, and in revised form, January 17, 2015 Published, JBC Papers in Press, February 9, 2015, DOI 10.1074/jbc.M115.636597

Daniel Bloch Hansen‡, Nestor Garrido-Comas§, Mike Salter¶, and Robert Fern‡1

From the ‡Plymouth University Peninsula Schools of Medicine and Dentistry, Plymouth PL6 8BU, the §Department of Cell Physiology and Pharmacology, University of Leicester, Leicester LE1 7RH, and the ¶Institute of Membrane and Systems Biology, University of Leeds, Leeds LS2 9JT, United Kingdom

Background: Astrocyte pH regulation is essential for brain function.
Results: Bicarbonate-independent acid load recovery in whole-mount astrocytes was achieved primarily via V-ATPase, which also held astrocytes at a basic resting pH.
Conclusion: V-ATPase is the major bicarbonate-independent H^+ extruder in a whole-mount astrocyte population.
Significance: High levels of V-ATPase expression will isolate astrocyte pH regulation from cytoplasm changes in other ion species.

The mechanisms of HCO_3^--independent intracellular pH (pH_i) regulation were examined in fibrous astrocytes within isolated neonatal rat optic nerve (RON) and in cultured cortical astrocytes. In agreement with previous studies, resting pH_i in cultured astrocytes was 6.82 ± 0.06 and inhibition of the V-ATPase H^+ pump by Cl^- removal or via the selective inhibitor bafilomycin had only a small effect upon resting pH_i and recovery following an acid load. In contrast, resting pH_i in RON astrocytes was 7.10 ± 0.04, significantly less acidic than that in cultured cells ($p < 0.001$), and responded to inhibition of V-ATPase with profound acidification to the 6.3–6.5 range. Fluorescent immuno-staining and immuno-gold labeling confirmed the presence V-ATPase in the cell membrane of RON astrocyte processes and somata. Using ammonia pulse recovery, pH_i recovery in RON astrocyte was achieved largely via V-ATPase with sodium-proton exchange (NHE) playing a minor role. The findings indicate that astrocytes in a whole-mount preparation such as the optic nerve rely to a greater degree upon V-ATPase for HCO_3^--independent pH_i regulation than do cultured astrocytes, with important functional consequences for the regulation of pH in the CNS.

Astrocytes are responsible for extracellular ion homeostasis in the CNS, including H^+. pH can have profound effects upon excitability, neurotransmission, and injury responses, and the mechanisms of pH regulation in astrocytes have been examined in detail previously. Acute intracellular pH (pH_i) balance in the CNS is determined by two factors: (i) the intrinsic buffering power of neural cells, and (ii) the activity of membrane transporters that move H^+ equivalents across cell membranes, resulting in cellular acid extrusion or acid loading (1–3). Acid extruders can either directly remove H^+ from cells or import HCO_3^-, whereas acid loaders are thought to exclusively remove HCO_3^-. Two HCO_3^--dependent transporters, the Na-HCO_3 cotransporter and the Na^+-driven Cl-HCO_3 exchanger, have been described in astrocytes (3, 4) in addition to an electroneutral Cl-HCO_3 exchanger (5). HCO_3^--independent transporters maintain intracellular pH by transporting H^+ either directly or coupled to another ionic gradient. Studies using cultured astrocytes indicate that the Na-H exchanger (NHE)[2] is the principal HCO_3^--independent H^+ extrusion protein in the CNS, coupling H^+ extrusion to the inward Na^+ gradient (3, 6–9). Astrocytes also express a V-type H-ATPase that can be blocked by bafilomycin, although the involvement of this pump in pH maintenance and recovery following an acid load is limited in cultured cells (10, 11).

The majority of information available regarding H^+ extrusion from astrocytes was obtained from culture preparations. These have the advantage of low background signal and ease of use but the disadvantage that the cells may behave differently from cells *in situ*, where they are integrated into complex neural networks. Using postnatal day 0–4 (P0–P4) rat optic nerves, we have now examined the involvement of V-ATPase and NHE in the maintenance of steady-state pH_i and pH_i recovery following an acid load in astrocytes. This white matter tract is premyelinated, allowing high-contrast imaging of ion-sensitive intracellular dyes, and contains a population of early maturing fibrous astrocytes. The nerve was transected at either end, and cells were imaged in the central region and are therefore in a native, effectively undamaged environment. We report that in contrast to cultured astrocytes, V-ATPase is the dominant HCO_3^--independent H^+ extrusion mechanism in this *in situ* astrocyte population.

* This work was supported by Biotechnology and Biological Sciences Research Council (BBSRC) Grant BB/J016969/1 (to R. F.).
⌘ *Author's Choice*—Final version full access.
◆ This article was selected as a Paper of the Week.
[1] To whom correspondence should be addressed: Plymouth University, Peninsula School of Medicine and Dentistry, John Bull Bldg., Research Way, Plymouth PL6 8BU, United Kingdom. Tel.: 44-1752-437365; E-mail: robert.fern@plymouth.ac.uk.

[2] The abbreviations used are: NHE, Na-H exchanger; BCECF, 2′,7′-bis-(2-carboxyethyl)-5 (and 6)-carboxyfluorescein; AM, acetoxymethyl; aCSF, artificial cerebrospinal fluid; GFAP, glial fibrillary acidic protein; NMDG, *N*-methyl-D-glucamine; EIPA, ethyl-isopropyl amiloride; RON, rat optic nerve; P, postnatal day(s).

EXPERIMENTAL PROCEDURES

Rat Optic Nerve Preparation—Postnatal day 0–2 (P0–P2) Lister Hooded or P0–P4 Wistar rats of both sexes were humanely killed, and the optic nerves were dissected according to regulations from the Home Office, United Kingdom, with approval from the local Animal Welfare and Ethical Review Board (AWERB) of the University of Leicester and Plymouth University. The nerves were placed in HEPES-buffered artificial cerebrospinal fluid (aCSF) (see below). The pH-sensitive fluorescent dye 2′,7′-bis-(2-carboxyethyl)-5 (and 6)-carboxyfluorescein (BCECF) (Molecular Probes Inc.) was used to measure pH_i. BCECF-AM (10 μM) was dissolved in dimethyl sulfoxide, 10% Pluronic acid, and cells were loaded in HEPES-aCSF at room temperature for 90 min (15 min for cultures). After washing, the ends of the nerves were fixed to a glass coverslip with a small amount of cyanoacrylate glue and sealed into a Plexiglas perfusion chamber with silicone grease (atmosphere chamber, Warner Instruments). The chamber was mounted on an Eclipse TE2000-U inverted microscope (Nikon), continuously superfused at a rate of 2 ml/min, and maintained in an oxygenated environment (see Ref. 12) for further details). The chamber temperature was maintained at 37 °C with a flow-through feedback tubing heater (Warner Instruments) positioned immediately before the chamber and a feedback objective heater (Bioptechs) that warmed the objective to 37 °C. This combination of heating systems regulated the temperature of the bath and coverslip to 37 °C, as established periodically with a temperature probe.

Astrocyte Cultures—Astrocytes were isolated and cultured using an established protocol (13). Brains from BALB/c mice embryos (embryonic days 14–16) were collected in Hanks' balanced salt solution (Gibco) on ice, and after removal of the meninges, the tissue was digested for 2 min at 37 °C with 2 ml of 1% trypsin solution. The digestion was stopped with 10 ml of DMEM (Gibco) with 10% FCS (Gibco). After washing, the tissue was triturated in 2 ml of 0.5% DNase solution. 10 ml of DMEM, 10% FCS medium was added, and cells were centrifuged for 5 min at 200 × *g*. The pellet was resuspended in DMEM, 10% FCS incubation media with 50 units/ml penicillin and 50 mg/ml streptomycin (P/S) (Invitrogen), and the cells were plated in poly-L-lysine (100 μg/ml) precoated flasks (1.8–3.5 × 10^7 cells/flask). The medium was partially exchanged every 3 days. After 15–20 days, a mixed glial culture was achieved. The cells were separated by shaking, leaving the astrocyte layer, which was washed twice with serum-free Hanks' balanced salt solution prior to trypsinization. Glial fibrillary acidic protein (GFAP) staining of sister cultures showed 93.9% of cells being $GFAP^+$. Astrocytes were centrifuged at 4 °C for 5 min at 200 × *g* and resuspended with incubation media DMEM, 10% FCS, P/S and plated on coverslips, which were incubated at 37 °C until mounted in an atmosphere chamber as described above.

Cell Imaging—Cells within the optic nerve or on coverslips were illuminated at 440 and 490 nm by a monochromator (Optoscan; Cairn Research), and images were collected every 30 s at 510 nm using an appropriate filter set (Chroma Technology) and a cooled CCD camera (CoolSNAP HQ; Roper Scientific). Cells were initially brought into focus during illumination at 490 nm, usually selecting a field containing >30 cells in optic nerves and >60 in astrocyte cultures. In the case of optic nerves, all the cells loading the dye at this age are astrocytes (12), and a typical optic nerve cell loading with BCECF is shown in Fig. 1*A*. The brightest 15 or 30 cells were selected for analysis to avoid data biasing between nerves or cultures, respectively. Once mounted in the microscope, nerves or cell cultures were left to equilibrate for 10–20 min in HEPES-aCSF to remove any unhydrolyzed dye before the start of each experiment. Regions of interest were drawn around individual cells, and following background subtraction, the fluorescence ratio for each was plotted against time.

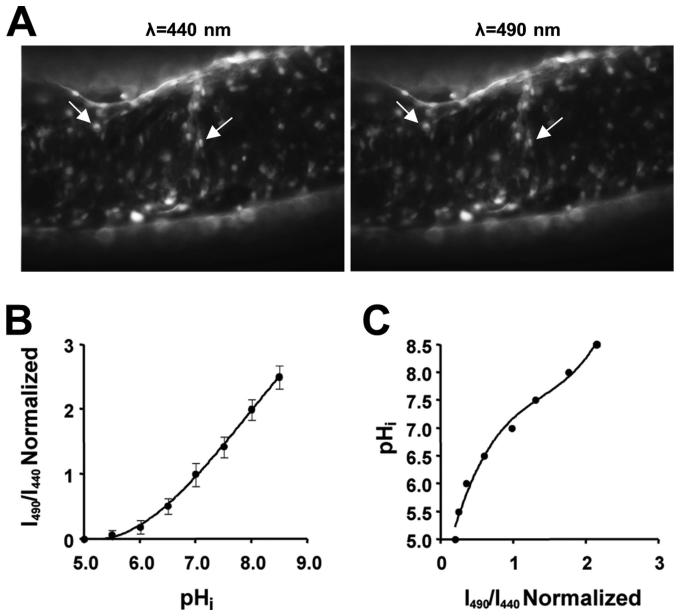

FIGURE 1. **Cell loading of BCECF-AM and pH_i calibration in optic nerve astrocytes.** *A*, images of BCECF-AM loading in rat optic nerve astrocytes. A large number of cells can be seen to have loaded the dye (*e.g. arrows*) during excitation at 440 and 490 nm. *B*, plot of the calibration curve obtained from optic nerve astrocytes. 490/440 ratios were obtained after exposing cells to high K^+/nigericin calibration solutions at pH values from 5.5 to 8.5. The 490/440 ratio was normalized to the ratio at pH 7.0. Values are given as mean ± S.E. *C*, replotted calibration curve with the data fitted to a third order polynomial function. This is used for correlating pH_i values to normalized 490/440 ratios obtained from single-point calibrations at the end of experiments.

Calibration—The 490/440 fluorescence ratio was calibrated against a lookup table giving a single point reference at the end of each experiment. The lookup table was produced by superfusing a series of optic nerves with a high K^+/nigericin solution driving pH_i to that of the superfusate and giving one point on a 490/440 *versus* pH_i plot (8, 14). The high K^+/nigericin solution contained (in mM): 10 Na^+, 130 K^+, 10 Cl^-, 130 gluconic acid, 0.6 Ca^{2+}, 0.6 $MgSO_4$, 10 glucose, and 10 PIPES for pH ≤ 6.8 or 10 HEPES for pH ≥ 7.0. For Nigericin (10 μM), gramicidin (5 μM), and ouabain (1 mM) solutions, pH was adjusted with NaOH, giving eight different solutions with pH ranging from 5.0 to 8.5 in intervals of 0.5. 490/440 ratios were calculated to obtain the calibration curve shown in Fig. 1*B*, normalized to pH 7.0. As in previous studies (8, 14), the calibration curve was replotted and fitted with a third order polynomial function obtaining a best-fit value R^2 of 0.98 (Fig. 1*C*). The 490/440 data from individual experiments was then converted to pH_i values

by exposing the cell to a pH 7.0 calibration solution at the end of each experiment, applying the resulting 490/440 value to the third order polynomial function and converting the whole data series using these values.

Acid Loading and H^+ Buffering—Rat optic nerves or astrocyte cultures were acid-loaded using the NH_4^+ prepulse technique (15). Briefly, nerves or cultures were prepared as described above and exposed to HEPES-aCSF containing 20 mM $(NH_4)_2SO_4$. NH_3 freely permeates the cell membrane and reacts with free H^+ in the cytoplasm, causing a rapid increase in pH_i. Slow NH_4^+ influx follows, acidifying the cell, and subsequent removal of the extracellular NH_3/NH_4^+ causes a rapid decrease in pH_i to below the starting value. Optic nerve astrocytes were exposed to NH_3/NH_4^+ for 5 min, whereas exposure time for cultured astrocytes was reduced to 2 min due to problems with cell viability. The shorter exposure time for cultured astrocytes allowed for a full recovery of pH_i consistent with Ref. 1. The shorter ammonia pulse also caused a smaller acidification and thus recovery over a narrowed band of pH_i values (6.6–7.0) as compared with optic nerve astrocytes.

H^+-buffering power was calculated using an established protocol (1, 8, 14). The total cellular H^+-buffering capacity ($\beta_{\mathbf{T}}$) is the product of an HCO_3-dependent component ($\beta_{HCO3} = 2.3\,[HCO_3^-]_i$) and an intrinsic component (β_i). By measuring the pH_i increases produced by exposing cells to different external concentrations of NH_4^+ under conditions where pH_i regulation is interrupted (8) and in the absence of HCO_3^-, $\beta_{\mathbf{T}} = \beta_i$, which can be calculated as

$$\beta_i = \Delta[NH_4^+]_i/\Delta pH_i \qquad \text{(Eq. 1)}$$

Nerves were initially superfused with HEPES-aCSF followed by HEPES-aCSF with Na^+ and Cl^- substituted to block pH regulation in the astrocytes (see below). Three rat optic nerves (RONs) were exposed to $[NH_4^+]$ in concentrations of 1, 2.5, 5, 10, or 20 mM. Following each pulse, pH_i, was extrapolated to time 0, $\Delta[NH_4^+]_i$ was calculated using the Henderson-Hasselbalch equation, and $\beta_{\mathbf{T}} = \beta_i$ was calculated and plotted against the resulting pH_i (4, 8).

Rat Optic Nerve Extracellular pH—Ion-sensitive microelectrodes were manufactured as described previously (16). Electrodes were pulled from glass capillaries (1.5-mm outer diameter, 0.86-mm inner diameter, Harvard Apparatus) with a Sutter model P-97 puller (Sutter Instrument Co.). Electrodes were salinized using *N*,*N*-dimethyltrimethylsilylamine (TMSDMA), backfilled with HEPES-aCSF (pH 7.45), and front-filled with the ion-exchange resin (hydrogen ionophore I: mixture A, Sigma-Aldrich). The reference electrode was pulled as above and filled with HEPES-aCSF. Experimental solutions were kept at 37 °C and continuously aerated. The Ag-AgCl bath electrode was connected to the superfusate using a 1 M KCl agar bridge to avoid drift in the Cl^--free solution. Dissected rat optic nerves were stored in HEPES-aCSF for at least 1 h to allow axon sealing. Nerves were then fixed onto coverslips as described above. Following impalement, the nerve was left to recover for 5–10 min before the start of experiments. The recordings were performed and recorded with a high impedance differential electrometer (FD223a, World Precision Instruments), a IX-228 data acquisition unit, and LabScribe2 software (both iWorx Systems, Inc.) with sampling at 1 Hz.

Due to differences in composition between electrode fillings and the experimental Na^+/Cl^--free HEPES-aCSF, we compensated for the junction potential by recording the change in junction potential in the chamber following experiments and subtracting it from the in-nerve recordings. The electrodes were calibrated using HEPES-aCSF with pH levels ± 1 unit relative to the control (6.4 and 8.4, respectively). pH sensitivity of the electrodes was found to be similar in control and Na^+/Cl^--free (NMDG gluconate-substituted) HEPES-aCSF.

Antibody Staining—Nerves were transferred to 0.1 M PBS prior to fixing in 4% paraformaldehyde for 30 min at room temperature. The nerves were then cryoprotected (20–30% sucrose for 5 min), transferred to Tissue-Tek medium (Sigma), and frozen using ethanol and dry ice. 20-μm sections were cut by cryostat and mounted onto microscope slides. The freshly cut sections were then submerged in 0.1 M PBS for 5 min and blocked in 0.1 M PBS containing 10% goat serum and 0.5% Triton-X for 120 min at room temperature prior to overnight exposure to primary antibody at 4 °C in the same solution. Monoclonal GFAP (Molecular Probes, 1:200) and rabbit anti-V-ATPase F (sc-20947, Santa Cruz Biotechnology, 1:100) were used. Slides were then washed (3 × 5 min) and incubated in the appropriate Alexa Fluor-conjugated secondary antibody (Molecular Probes, 1:1000) for 60 min at room temperature. The sections were then washed sequentially in 0.5, 0.1, and 0.05 M PBS containing 10% normal serum. Images were collected using an Olympus IX70 confocal microscope (60× objective). In all cases, controls treated as above but without primary antibody were blank.

Electron Microscopy—Optic nerves were post-fixed in 3% glutaraldehyde/Sorenson's Ringer prior to post-fixing with 2% osmium tetroxide and dehydration prior to infiltration in epoxy. Sections were counterstained with uranyl acetate and lead citrate and examined with a Jeol 100CX electron microscope (see Ref. 17 for details). For post-embedding immunolabeling, primary antibody was applied to the sections overnight, and appropriate 20-nm gold particle secondary antibodies were applied following washing (see Ref. 18 for further details).

Solutions and Chemicals—HEPES-buffered aCSF contained (in mM): 126 NaCl, 4 KCl, 2 NaH_2PO_4, 2 $MgSO_4$, 25 HEPES, 10 glucose, 2 calcium gluconate, 2 sodium cyclamate, pH 7.45, adjusted with HCl. For Na^+-free HEPES-buffered aCSF, NaCl was replaced by 128 mM NMDG Cl^- and 2 mM KCl was replaced by 2 mM KH_2PO_4, omitting both sodium cyclamate and NaH_2PO_4. For Cl^--free aCSF, NaCl was replaced by 128 mM sodium cyclamate, and KCl was replaced by 2 mM K^+ gluconate and 2 mM KH_2PO_4. The Na^+- and Cl^--free solution contained (in mM) 2 $MgSO_4$, 25 HEPES, 10 glucose, 2 calcium gluconate, 2 potassium gluconate, 2 KH_2PO_4, and 130 NMDG gluconate prepared by titrating the NMDG-containing solution with gluconate to pH 7.45. Osmolarity for all solutions was measured using a vapor pressure osmometer (Camlab) and adjusted with sucrose to 315 mosM. All chemicals were purchased from Sigma-Aldrich) unless otherwise stated.

Statistics—Static significance was tested using one-way analysis of variance with Bonferroni's post hoc test or Student's *t* test as appropriate (GraphPad, Prism).

RESULTS

Na^+- and Cl^--dependent pH_i Regulation Differs between in Situ and Cultured Astrocytes—We determined the contribution of the Cl^--dependent V-ATPase to resting pH_i levels in both cultured astrocytes and *in situ* rat optic nerve astrocytes. Optic nerve and cultured astrocytes superfused for 15–25 min with HEPES-aCSF displayed baseline pH_i of 7.10 ± 0.04 ($n = 4$ optic nerves, 60 cells) and 6.82 ± 0.06 ($n = 4$ cultures, 90 cells), respectively ($p < 0.01$; Fig. 2, *A* and *C*). Cl^- removal did not significantly affect the pH_i of cultured astrocytes, which fell to 6.71 ± 0.07 ($p > 0.05$; $n = 60$; Fig. 2, *A* and *C*), whereas pH_i in optic nerve astrocytes fell significantly to 6.30 ± 0.04 ($p < 0.001$; $n = 4$ optic nerves, 60 cells; Fig. 2, *A* and *C*). Perfusion with the selective V-ATPase inhibitor bafilomycin (50 nM) reduced optic nerve astrocyte resting pH_i to 6.52 ± 0.02 ($p < 0.01$;c Fig. 2, *B* and *C*) over a similar 20–30-min time course to the acidification produced by Cl^- removal. Bafilomycin reduced pH_i in cultured astrocytes by ~0.15 pH units to 6.64 ± 0.04 ($n = 4$ cultures, 90 cells), which was significantly less than the ~0.61 pH unit change found in optic nerve astrocytes. The plateau pH_i levels in optic nerve and cultured astrocytes exposed to bafilomycin were not significantly different ($p > 0.5$), and V-ATPase activity in optic nerve cells therefore accounts for their alkaline resting pH_i as compared with cultured cells. To confirm the Cl^--dependent nature of the V-ATPase activity in optic nerve astrocyte, pH_i recovery following a 30-min period of 0 Cl^- perfusion was shown to be blocked by bafilomycin upon Cl^- restoration (Fig. 2*D*).

The differential effect of V-ATPase inhibition between cultured and *in situ* astrocytes suggests higher rates of H^+ extrusion via this route in optic nerve astrocytes. Following an acid load (exposure to a 20 mM ammonia pulse) in cultured astrocytes, pH_i fell from a baseline of 6.98 ± 0.05 to 6.60 ± 0.07 before recovering over a 7-min period (Fig. 2*E*, *segment c-d*) to 6.96 ± 0.07 ($p > 0.05$ *versus* baseline; $n = 4$ cultures, 90 cells). Na^+ removal largely abolished the pH_i recovery following an acid load, with pH_i reaching 6.69 ± 0.07 ($n = 4$ cultures, 90 cells; Fig. 2*F*), which is consistent with prior studies that report largely Na^+-dependent forms of HCO_3^--independent acid extrusion in these cells (8, 9). In contrast, removal of Cl^- from the medium had no significant effect upon pH_i recovery in cultured astrocytes (Fig. 2*F*).

V-ATPase Is the Principal Acid Extrusion Mechanisms in Optic Nerve Astrocytes—We determined the Na^+ and Cl^- dependence of acid extrusion in optic nerve astrocytes, using ammonia pulse recovery. Baseline pH_i was 7.14 ± 0.08 ($n = 4$ optic nerves, 60 cells), and following the acid load, pH_i did not fully recover, returning to a mean of 6.81 ± 0.07 ($p < 0.001$, Fig. 3*A*). The recovery from an acid load in Cl^--free medium was significantly reduced in optic nerve astrocytes, reaching a plateau pH_i of 6.36 ± 0.16 ($p < 0.001$ *versus* control), whereas pH_i recovered to 6.78 ± 0.12 in Na^+-free medium ($p < 0.001$ *versus* Cl^--free; $n = 4$ nerves, 60 cells, Fig. 3*B*) after 20 min. Following ammonia loading, perfusion with the NHE inhibitor EIPA resulted in pH_i recovery to 6.76 ± 0.10 ($n = 4$ nerves, 60 cells; Fig. 3*C*), comparable with the recovery in Na^+-free medium ($p > 0.89$). In the presence of the V-ATPase inhibitor bafilomycin, pH_i recovery reached a steady value of 6.57 ± 0.13 (Fig. 3*D*, $n = 4$ optic nerves, 60 cells), not significantly different from that obtained in Cl^--free medium ($p > 0.31$). A combination of EIPA + Cl^--free medium (Fig. 3*E*) or bafilomycin + Na^+-free medium (Fig. 3*F*) prevented pH_i recovery following an acid load.

pH_i recovery rates calculated for the 5-min period following the removal of ammonia confirm the significance of V-ATP in

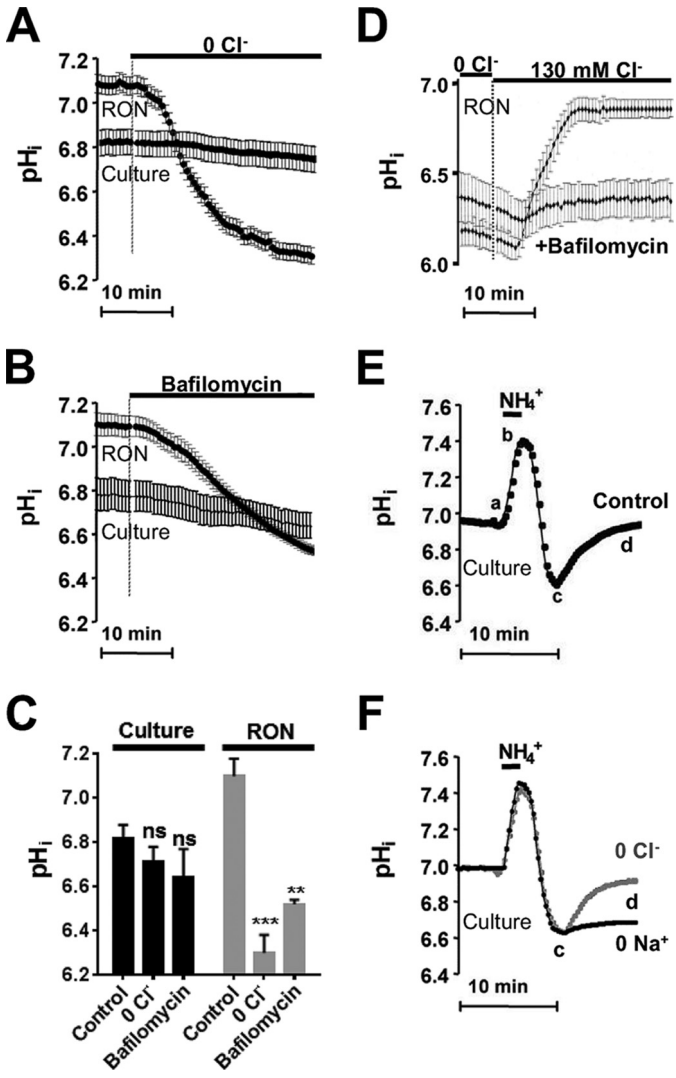

FIGURE 2. **The effect of bafilomycin or ionic substitution upon HCO_3^--independent pH_i in rat optic nerve and cultured astrocytes.** *A*, substitution of Cl^- (0 Cl^-) in HEPES-buffered, nominally HCO_3^--free, aCSF evokes a large acidification in RON astrocytes, but not in cultured astrocytes (*Culture*). *B*, exposure to the V-ATP blocker bafilomycin (50 nM) evokes a large acidification in optic nerve astrocytes but not in cultured astrocytes. *C*, summary of data in *A* and *B*. Values are given as mean ± S.E. Significance is given relative to the respective control: **, $p < 0.001$, ***, $p < 0.0001$. *ns*, not significant. *D*, pH_i of optic nerve astrocytes acidified by Cl^- removal is normalized following restoration of physiological extracellular Cl^- in a bafilomycin-sensitive fashion. *E*, recovery of pH_i from an acid load in cultured astrocytes in control solution. Baseline pH_i was stable prior to the onset of a 2 min 20 mM ammonia pulse. *Segment a-b* is the alkalinization evoked by NH_4 exposure, *segment b-c* is the acid load generated after switching back to ammonia-free conditions, and *segment c-d* is the pH_i recovery. *F*, as in E; pH_i recovery in cultured astrocytes was reduced in the absence of extracellular Na^+ (0 Na^+) but unaffected by Cl^- substitution (0 Cl^-).

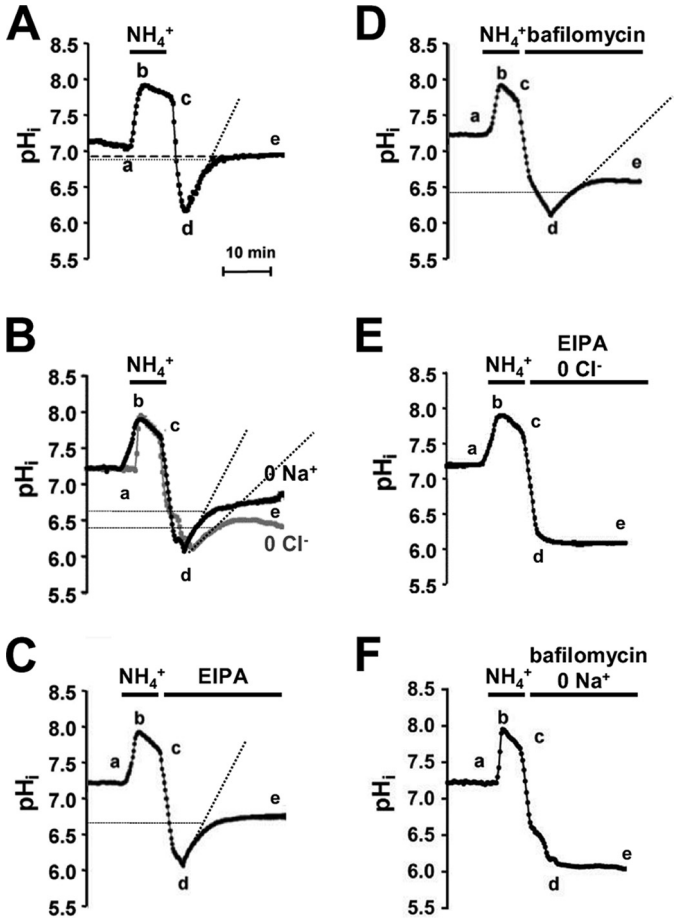

FIGURE 3. **HCO_3^--independent H^+ extrusion in neonatal optic nerve astrocytes.** *A*, mean pH_i changes in HEPES-aCSF following a 5-min 20 mM ammonia pulse (*segment a-c*). pH_i recovered after return to ammonia-free conditions (*segment d-e*), but not completely (note *thick dashed line*). *B*, as in A; the recovery was reduced by removal of extracellular Na^+ (0 Na^+) and Cl^- (0 Cl^-). *C* and *D*, mean pH_i recovery following acid load in the presence of the Na-H exchange inhibitor EIPA or the V-ATPase inhibitor bafilomycin. Both inhibitors reduced the recovery, although bafilomycin reduced it to the greatest extent. *E* and *F*, pH_i recovery was prevented by the following combinations: NHE inhibitor EIPA and Cl^- removal or V-ATPase inhibitor bafilomycin combined with Na^+ removal. *Dotted lines* on *A–D* indicate recovery rates within the first 5 min following removal of NH_4^+. All values are given as mean ± S.E.

optic nerve astrocytes. The rate in control HCO_3^--free conditions was 0.15 pH units/min, whereas recovery in the absence of NHE (0 Na^+ or EIPA) or V-ATPase activity (0 Cl^- or bafilomycin) was 0.12 and 0.07 pH units/min, respectively. These results demonstrate that V-ATPase, in addition to maintaining resting pH_i, is the major contributor to acid extrusion following an acidic challenge in optic nerve astrocytes.

Immuno-staining showed co-expression of V-ATPase and the astrocyte marker GFAP, confirming the presence of significant V-ATPase expression in neonatal optic nerve astrocytes (Fig. 4*A*). At the ultrastructural level, immuno-gold labeling of V-ATPase revealed that the protein was present in the cell membrane of astrocyte processes neighboring axons (Fig. 4, *B* and *C*) and in astrocyte somata (Fig. 4*D*), in addition to the previously documented staining of axonal vesicular tubular complex (18). The contribution of V-ATPase to pH_i regulation in these cells was therefore not a result of H^+ loading into glial synaptic-type vesicles.

Buffering Capacity and Extracellular pH—The buffering capacity of astrocyte *in situ* has never been assessed, and calculation of the buffering capacity requires displacement of pH_i by known acid loads in the absence of active pH regulation. This is generally achieved by exposure to various NH_4^+ concentrations, and the calculation hereof requires knowledge of both pH_i and extracellular pH (pH_o). pH_i regulation was eliminated in optic nerve astrocytes by removal of Na^+ and Cl^-, producing a decrease in pH_i from the resting point of 7.15 to 6.07 ± 0.02 ($p < 0.001$; $n = 4$ nerves, 60 cells, Fig. 5*A*). pH_o in neonatal rat optic nerve superfused with HEPES-buffered aCSF (pH 7.45) deviated from that of the bath due to the presence of diffusion barriers between the two compartments and was recorded as 7.28 ± 0.02 ($n = 4$ nerves) using ion-sensitive microelectrodes (Fig. 5*B*). Perfusion with 0 Na^+/0 Cl^- produced a small alkaline increase in the nerve extracellular space to pH 7.36 ± 0.02 ($n = 4$, $p < 0.05$, Fig. 5*B*). Following interruption of pH_i regulation by the ionic substitution, optic nerve astrocytes were acid-loaded with NH_4^+ at various concentrations (8) (Fig. 5, *A* and *C*), and the intrinsic buffering capacity (β_i) was calculated (see "Experimental Procedures"). There was a non-linear relation between β_i and pH_i with a maxima around pH 6.5.

DISCUSSION

The ease with which mammalian astrocyte cultures can be generated and the control the preparation allows of the extracellular medium have resulted in a particular focus on the physiological properties of these cells. When it comes to ion homeostasis, cell culture studies have revealed the range of transport proteins that astrocytes can express and the physiological functions that they can perform. The list of pH-regulating membrane proteins identified in this way includes NHE, Na-HCO_3 cotransport, Na^+-driven Cl-HCO_3 exchange, Cl-HCO_3 exchange, and a V-ATPase, most of which have also been functionally identified in lower animal preparations (see Refs. 2 and 3 for reviews). The few studies of pH regulation in mammalian astrocytes *in vivo* or in whole-mount preparations indicate the presence of Na-HCO_3 cotransport in adult retinal astrocytes (19) and of Na-HCO_3 cotransport and NHE in P8–20 medullary astrocytes (20). The current investigation is the first to examine the contribution made by the transporters NHE and V-ATPase in the nominal absence of HCO_3^- in a whole-mount astrocyte population, revealing the predominance of V-ATPase, a finding with significant functional implications for CNS pH handling.

Neonatal White Matter Astrocytes—The white matter astrocyte population in the CNS matures early relative to other neural cell types. Arising from progenitor cells, including radial glia (21, 22), mature phenotype $GFAP^+$ astrocytes are present in the human fetal brain from about post-conception weeks 11 to 14 (23), and populate the intermediate zone that will ultimately form cortical white matter from post-conception weeks 16 to 18 (24). Fibrous white matter astrocytes are established particularly early; for example, they appear in the cortex before protoplasmic gray matter astrocytes (24, 25). Studies of astrocyte development in central white matter are complicated by the complex morphological arrangement of axon tracts at different maturational stages. Large differences in astrocyte develop-

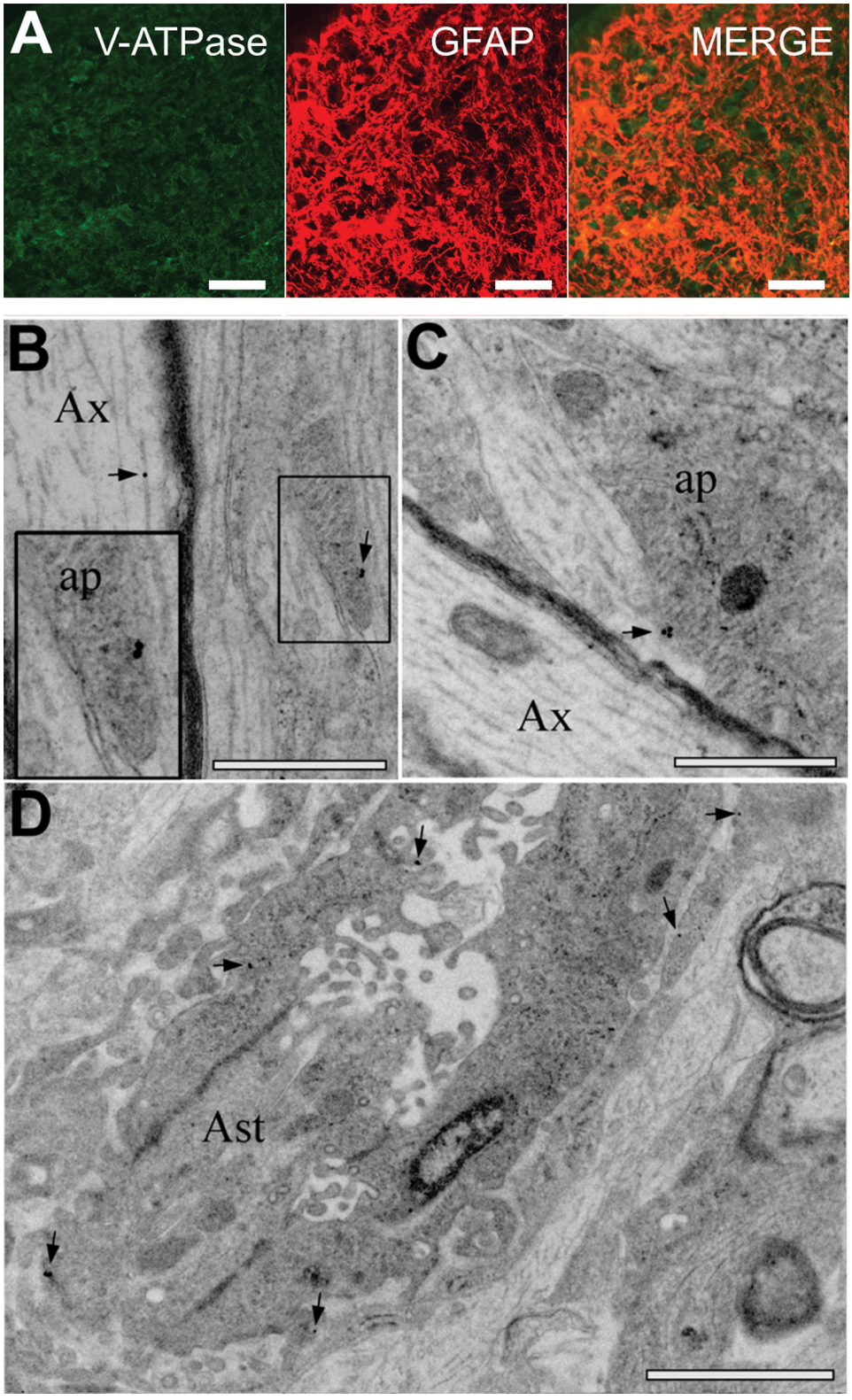

FIGURE 4. **V-ATPase expression in P2 rat optic nerve.** *A*, V-ATPase (*green*, *left*), and GFAP (*middle*, *red*) expression in the same section, overlaid on the *right*. Note the clear astrocytic expression of V-ATPase, in addition to expression between astrocytes that may correspond to axonal protein. *B–D*, immuno-gold labeling of electron micrographs for V-ATPase reactivity in the long section, showing gold particles (*arrows*) localized to the membrane of astrocyte processes (*ap*, *B* and *C*), and somata (*Ast*, *D*). Note that axons (*Ax*) also contain particles. Note the presence of glial filaments in the astrocyte processes and the wide-bore endoplasmic reticulum, dark bodies, and glycogen particles in the somata (see Ref. 17). The *box* in *B* is shown at higher magnification. *Scale bars* = 10 μm in A; 500 nm in *B* and *C*; and 1 μm in *D*.

ment have been noted, for example, between closely apposed fiber tracts in the optic radiations (24). These complications are avoided in the optic nerve, which is a uniform and structurally isolated white matter tract where astrocytes are generated from astrocyte precursor cells rather than by transformation of radial glia (26–29). By mid-gestation in humans, optic nerve astrocyte

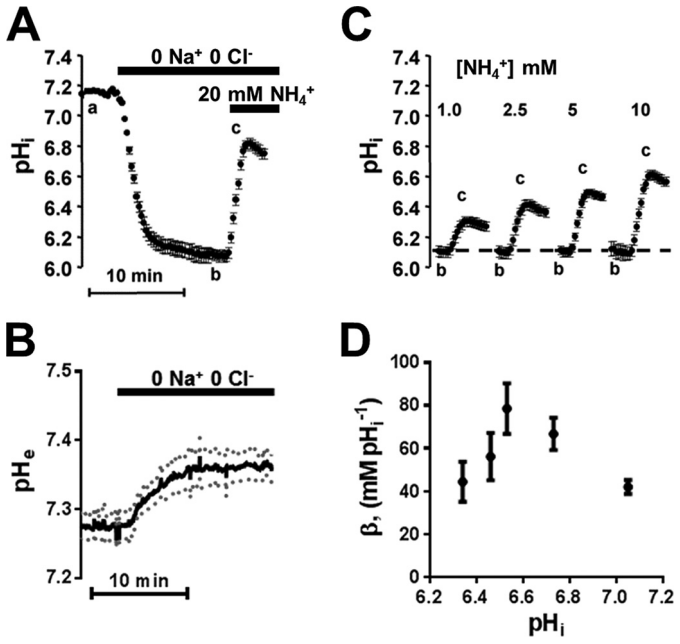

FIGURE 5. **Intrinsic buffering capacity and pH_o were determined following blockade of Na-H exchange and V-ATPase acid extrusion by NMDG gluconate substitution of Na^+ and Cl^-.** *A*, Na^+ and Cl^- removal produced a 1.08 ± 0.08 pH units acidification in optic nerve astrocytes, and exposure to NH_4^+ (20 mM) in the absence of acid extrusion mechanisms evoked an alkalinization. *B*, pH_o measured in optic nerve using ion-sensitive microelectrodes was increased by 0.08 pH units following Na^+ and Cl^- removal. *C* and *D*, exposure to NH_4^+ as in *A* (1–10 mM) resulted in increasing alkalinization. The buffering capacity (β_i) for each [NH_4^+] concentration was calculated and plotted against the resulting pH_i. Note that the pH change has been extrapolated back to time 0 for each solution. All values are given as mean ± S.E.

maturation is largely complete, predating the onset of myelination by ~20 weeks (26).

In animal studies, astrocyte precursor cells populate the RON at fetal day 17, and $GFAP^+$ astrocytes are generated continually until the end of the first week of life (27–29). At birth, >70% of cells in the RON are astrocytes with many of the features of mature cells including a radiating stellate morphology, expression of glial filaments, and organelle structures typical of the mature phenotype (such as endoplasmic reticulum, mitochondria, and Golgi). These astrocytes selectively accumulate AM-conjugated dyes (12), and the current study has taken advantage of the early maturation of fibrous astrocytes to examine pH_i regulation in an effectively intact whole-mount preparation.

Astrocytes in Situ Rely Primarily on V-ATPase for HCO_3^--independent pH_i Regulation—V-ATPase is thought to be present in nearly every eukaryotic cell, where it acidifies intracellular organelles such as lysosomes, secretory, and synaptic vesicles. In the plasma membrane, V-ATPase functions to acidify the extracellular space, facilitating nephronal acidification, resorption of bone by osteoclasts, or reabsorption of bicarbonate in renal proximal tubules (reviewed in Refs. 32 and 33). In the absence of HCO_3^-, NHE1 has been identified as the principal acid extrusion mechanism in astrocytes (10, 30, 31) (see Ref. 3 for review), with V-ATPase being a minor contributor in cultured rat hippocampal astrocytes (10) and not involved in baseline pH_i maintenance in cultured cortical astrocytes (30). V-ATPase is dependent upon extracellular [Cl^-] (34–36), and consistent with the low activity of V-ATPase in cultures, we found only a minor change in pH_i of cultured astrocytes upon Cl^- removal or block by the selective inhibitor bafilomycin. In optic nerve astrocytes, these conditions resulted in significant acidification, leading to a pH_i convergence in the two astrocyte populations. HCO_3^--independent pH recovery in cultured astrocytes was unaffected by Cl^- removal, but was highly Na^+-dependent. These findings align with data on astrocyte cultures showing that H^+ extrusion in HEPES-buffered medium at a pH_i of 6.05 is mediated by EIPA- and amiloride-sensitive NHE (8). In comparison, pH recovery from an acid load in optic nerve astrocytes exhibited little Na^+ or EIPA sensitivity, whereas Cl^- removal or bafilomycin greatly reduced acid extrusion. These data are consistent with the hypothesis that HCO_3^--independent pH_i regulation in optic nerve astrocytes is mediated predominantly by V-ATPase with NHE playing a minor role. Consistent with this hypothesis, immuno-staining at the light and ultrastructural levels shows robust V-ATPase expression in the cell membrane of these astrocytes.

Buffering Capacity of Astrocytes in Situ—Buffering power in cultured cerebral and hippocampal astrocytes is essentially constant in the pH range 6–7 (37, 38) or linearly decreases with increasing pH_i (8, 31). We found a non-linear relation between buffering power and pH_i in optic nerve astrocytes. Measurements of buffering power are inherently variable, especially at low pH values (*e.g.* Ref. 31), and any inferred linear relationship with pH is possibly unwarranted. Buffering power distribution is the sum of the concentration and pK_a of all proton-buffering molecules in the cell (39); the buffering distribution therefore depends on the cellular composition and will not necessarily follow pH linearly.

We found that the intrinsic buffering capacity of the optic nerve astrocytes was above 40 mM $(pH)^{-1}$ throughout the pH range ~6.3–7.1. This is in the 26–50 mM $(pH)^{-1}$ range found in hippocampal slices, whole-brain cortical tissue homogenate, and isolated synaptosomes (37, 40–42), but substantially greater than the 10.5–14.1 mM $(pH)^{-1}$ range of cultured astrocytes (8, 31, 38). It is possible that buffering capacity is generally reduced in cultured cells as compared with cells *in vivo*. A high intrinsic buffering capacity paired with a presumably higher bicarbonate buffering power due to the elevated resting pH_i of *in situ* astrocytes would render the cells more resistant to pH fluctuations than their cultured counterparts.

Conclusion—Excitability in the neonatal rat optic nerve is mediated by long-duration, slow-conducting action potentials (43), and excitability-dependent changes in the extracellular space are exaggerated in this tissue. Extracellular [K^+] can rise ~20 mM during electrical stimulation of neonatal optic nerve axons (44), and neighboring astrocytes express relatively high levels of voltage-gated Na^+ channels, which are down-regulated in the absence of axonal contact (45). Large activity-dependent elevations in extracellular [K^+] are likely to evoke significant rises in intracellular [Na^+] in these astrocytes, which would influence pH_i regulation mediated via NHE. This astrocyte population may therefore require a form of pH_i regulation that is independent of intracellular [Na^+], such as that provided by V-ATPase. Reliance upon V-ATPase for HCO_3^--independent pH_i regulation, in contrast to NHE, may therefore have

functional utility for neonatal white matter astrocytes. However, the assumption that CNS astrocytes in general express low levels of V-ATPase and high levels of NHE is based almost entirely upon cell culture studies, and the current findings question the validity of this assumption. Voltage-gated Na^+ channels and Na^+-dependent transport expression are widespread among astrocyte populations, and intracellular [Na^+] has recently been implicated in the regulation of astrocyte signaling at synapses (46). Synapses are also sites where pH_i regulation is an essential function of astrocyte processes; for example, activity-dependent acidification at NMDA-type glutamate receptors would have profound consequences for synaptic integration (47). Na^+-independent pH_i regulation may therefore be a general requirement for perisynaptic astrocyte processes. Because astrocytes *in vitro* do not form processes that are integrated into a neural network, they may fail to express the levels of V-ATPase found in the current study.

In general, astrocytes expressing high levels of V-ATPase will have an elevated capacity for pH_i regulation, in particular at the acid pH levels that prevail under ischemic conditions in the CNS. These are conditions under which such a transporter might be required because HCO_3^- levels will be reduced, limiting HCO_3^--dependent pH_i regulation, whereas NHE is unlikely to function efficiently due to reduced extracellular pH (3). In this regard, it is interesting that astrocytes contain the only significant energy reserve in the CNS in the form of glycogen (48), and V-ATPase may therefore participate in pH maintenance during limited periods of ischemia. High levels of functional V-ATPase expression in astrocytes therefore may have important implications for both the physiology and the pathophysiology of the CNS.

REFERENCES

1. Roos, A., and Boron, W. F. (1981) Intracellular pH. *Physiol. Rev.* **61,** 296–434
2. Deitmer, J. W., and Rose, C. R. (1996) pH regulation and proton signalling by glial cells. *Prog. Neurobiol.* **48,** 73–103
3. Chesler, M. (2003) Regulation and modulation of pH in the brain. *Physiol. Rev.* **83,** 1183–1221
4. Bevensee, M. O., Apkon, M., and Boron, W. F. (1997) Intracellular pH regulation in cultured astrocytes from rat hippocampus. II. Electrogenic Na/HCO_3 cotransport. *J. Gen. Physiol.* **110,** 467–483
5. Shrode, L. D., and Putnam, R. W. (1994) Intracellular pH regulation in primary rat astrocytes and C6 glioma cells. *Glia* **12,** 196–210
6. Boyarsky, G., Ransom, B., Schlue, W. R., Davis, M. B., and Boron, W. F. (1993) Intracellular pH regulation in single cultured astrocytes from rat forebrain. *Glia* **8,** 241–248
7. Pizzonia, J. H., Ransom, B. R., and Pappas, C. A. (1996) Characterization of Na^+/H^+ exchange activity in cultured rat hippocampal astrocytes. *J. Neurosci. Res.* **44,** 191–198
8. Bevensee, M. O., Weed, R. A., and Boron, W. F. (1997) Intracellular pH regulation in cultured astrocytes from rat hippocampus. I. Role Of HCO_3. *J. Gen. Physiol.* **110,** 453–465
9. Cengiz, P., Kintner, D. B., Chanana, V., Yuan, H., Akture, E., Kendigelen, P., Begum, G., Fidan, E., Uluc, K., Ferrazzano, P., and Sun, D. (2014) Sustained Na^+/H^+ exchanger activation promotes gliotransmitter release from reactive hippocampal astrocytes following oxygen-glucose deprivation. *PLoS One* **9,** e84294
10. Pappas, C. A., and Ransom, B. R. (1993) A depolarization-stimulated, bafilomycin-inhibitable H^+ pump in hippocampal astrocytes. *Glia* **9,** 280–291
11. Philippe, J. M., Dubois, J. M., Rouzaire-Dubois, B., Cartron, P. F., Vallette, F., and Morel, N. (2002) Functional expression of V-ATPases in the plasma membrane of glial cells. *Glia* **37,** 365–373
12. Fern, R. (1998) Intracellular calcium and cell death during ischemia in neonatal rat white matter astrocytes *in situ*. *J. Neurosci.* **18,** 7232–7243
13. McCarthy, K. D., and de Vellis, J. (1980) Preparation of separate astroglial and oligodendroglial cell cultures from rat cerebral tissue. *J. Cell Biol.* **85,** 890–902
14. Boyarsky, G., Ganz, M. B., Sterzel, R. B., and Boron, W. F. (1988) pH regulation in single glomerular mesangial cells. I. Acid extrusion in absence and presence of HCO_3. *Am. J. Physiol.* **255,** C844–C856
15. Boron, W. F., and De Weer, P. (1976) Intracellular pH transients in squid giant axons caused by CO_2, NH_3, and metabolic inhibitors. *J. Gen. Physiol.* **67,** 91–112
16. Voipio, J., Pasternack, M., and MacLeod, K. T. (1994) Ion-sensitive microelectrodes. in *The Plymouth Workshop Handbook* (Ogden, D., ed), pp. 275–316, The Company of Biologists, Cambridge, UK
17. Thomas, R., Salter, M. G., Wilke, S., Husen, A., Allcock, N., Nivison, M., Nnoli, A. N., and Fern, R. (2004) Acute ischemic injury of astrocytes is mediated by Na-K-Cl cotransport and not Ca^{2+} influx at a key point in white matter development. *J. Neuropathol. Exp. Neurol.* **63,** 856–871
18. Alix, J. J., Dolphin, A. C., and Fern, R. (2008) Vesicular apparatus, including functional calcium channels, are present in developing rodent optic nerve axons and are required for normal node of Ranvier formation. *J. Physiol.* **586,** 4069–4089
19. Newman, E. A. (1999) Sodium-bicarbonate cotransport in retinal astrocytes and Muller cells of the rat. *Glia* **26,** 302–308
20. Erlichman, J. S., Cook, A., Schwab, M. C., Budd, T. W., and Leiter, J. C. (2004) Heterogeneous patterns of pH regulation in glial cells in the dorsal and ventral medulla. *Am. J. Physiol. Regul. Integr. Comp. Physiol.* **286,** R289–R302
21. Freeman, M. R. (2010) Specification and morphogenesis of astrocytes. *Science* **330,** 774–778
22. Howard, B. M., Zhicheng, M. o., Filipovic, R., Moore, A. R., Antic, S. D., and Zecevic, N. (2008) Radial glia cells in the developing human brain. *Neuroscientist* **14,** 459–473
23. Wierzba-Bobrowicz, T., Lechowicz, W., and Kosno-Kruszewska, E. (1997) A morphometric evaluation of morphological types of microglia and astroglia in human fetal mesencephalon. *Folia Neuropathol.* **35,** 29–35
24. Roessmann, U., and Gambetti, P. (1986) Astrocytes in the developing human brain. An immunohistochemical study. *Acta Neuropathol.* **70,** 308–313
25. Takashima, S., and Becker, L. E. (1983) Developmental changes of glial fibrillary acidic protein in cerebral white matter. *Arch. Neurol.* **40,** 14–18
26. Sturrock, R. R. (1975) A light and electron microscopic study of proliferation and maturation of fibrous astrocytes in the optic nerve of the human embryo. *J. Anat.* **119,** 223–234
27. Vaughn, J. E. (1969) An electron microscopic analysis of gliogenesis in rat optic nerves. *Z. Zellforsch. Mikrosk. Anat.* **94,** 293–324
28. Skoff, R. P., Price, D. L., and Stocks, A. (1976) Electron microscopic autoradiographic studies of gliogenesis in rat optic nerve. II. Time of origin. *J. Comp. Neurol.* **169,** 313–334
29. Mi, H., and Barres, B. A. (1999) Purification and characterization of astrocyte precursor cells in the developing rat optic nerve. *J. Neurosci.* **19,** 1049–1061
30. Amos, B. J., and Chesler, M. (1998) Characterization of an intracellular alkaline shift in rat astrocytes triggered by metabotropic glutamate receptors. *J. Neurophysiol.* **79,** 695–703
31. McLean, L. A., Roscoe, J., Jorgensen, N. K., Gorin, F. A., and Cala, P. M. (2000) Malignant gliomas display altered pH regulation by NHE1 compared with nontransformed astrocytes. *Am. J. Physiol. Cell Physiol.* **278,** C676–C688
32. Beyenbach, K. W., and Wieczorek, H. (2006) The V-type H^+ ATPase: molecular structure and function, physiological roles and regulation. *J. Exp. Biol.* **209,** 577–589
33. Breton, S., and Brown, D. (2013) Regulation of luminal acidification by the V-ATPase. *Physiology* **28,** 318–329
34. Kaunitz, J. D., Gunther, R. D., and Sachs, G. (1985) Characterization of an electrogenic ATP and chloride-dependent proton translocating pump from rat renal medulla. *J. Biol. Chem.* **260,** 11567–11573

35. Fernández, R., and Malnic, G. (1998) H^+ ATPase and Cl^- interaction in regulation of MDCK cell pH. *J. Membr. Biol.* **163,** 137–145
36. Malnic, G., and Geibel, J. P. (2000) Cell pH and H^+ secretion by S3 segment of mammalian kidney: role of H^+-ATPase and Cl^-. *J. Membr. Biol* **178,** 115–125
37. Katsura, K., Mellergård, P., Theander, S., Ouyang, Y. B., and Siesjö, B. K. (1993) Buffer capacity of rat cortical tissue as well as of cultured neurons and astrocytes. *Brain Res.* **618,** 283–294
38. Pappas, C. A., and Ransom, B. R. (1994) Depolarization-induced alkalinization (DIA) in rat hippocampal astrocytes. *J. Neurophysiol.* **72,** 2816–2826
39. Boron, W. F. (2004) Regulation of intracellular pH. *Adv. Physiol. Educ.* **28,** 160–179
40. Jean, T., Frelin, C., Vigne, P., Barbry, P., and Lazdunski, M. (1985) Biochemical properties of the Na^+/H^+ exchange system in rat brain synaptosomes. Interdependence of internal and external pH control of the exchange activity. *J. Biol. Chem.* **260,** 9678–9684
41. Nachshen, D. A., and Drapeau, P. (1988) The regulation of cytosolic pH in isolated presynaptic nerve terminals from rat brain. *J. Gen. Physiol.* **91,** 289–303
42. Roberts, E. L., Jr., and Chih, C. P. (1998) The pH buffering capacity of hippocampal slices from young adult and aged rats. *Brain Res.* **779,** 271–275
43. Foster, R. E., Connors, B. W., and Waxman, S. G. (1982) Rat optic nerve: electrophysiological, pharmacological and anatomical studies during development. *Brain Res.* **255,** 371–386
44. Ransom, B. R., Yamate, C. L., and Connors, B. W. (1985) Activity-dependent shrinkage of extracellular space in rat optic nerve: a developmental study. *J. Neurosci.* **5,** 532–535
45. Minturn, J. E., Sontheimer, H., Black, J. A., Ransom, B. R., and Waxman, S. G. (1992) Sodium channel expression in optic nerve astrocytes chronically deprived of axonal contact. *Glia* **6,** 19–29
46. Kirischuk, S., Parpura, V., and Verkhratsky, A. (2012) Sodium dynamics: another key to astroglial excitability? *Trends Neurosci.* **35,** 497–506
47. Traynelis, S. F., and Cull-Candy, S. G. (1991) Pharmacological properties and H^+ sensitivity of excitatory amino acid receptor channels in rat cerebellar granule neurones. *J. Physiol.* **433,** 727–763
48. Ransom, B. R., and Fern, R. (1997) Does astrocytic glycogen benefit axon function and survival in CNS white matter during glucose deprivation? *Glia* **21,** 134–141